# Novel techniques for the optical characterization of photovoltaic materials and devices

P. Maddalena[a],*, A. Parretta[b], A. Sarno[b], P. Tortora[a]

[a] INFM, Dipartimento di Scienze Fisiche, Università di Napoli "Federico II", Complesso Universitario di Monte S. Angelo, Via Cintia, I-80126 Napoli, Italy
[b] Centro Ricerche ENEA, Località Granatello, C.P. 32, I- 80055 Portici (NA), Italy

## Abstract

By means of newly designed optical instrumentation, mainly based on the use of integrating spheres, the fundamental optical properties of photovoltaic materials and devices (solar cells, modules) have been investigated. Relevant results concerned the optical loss (reflectance) of devices and the transmittance of semitransparent materials, used in the window sheets, under both direct and diffuse light. All the developed techniques are non-destructive and allow the characterization of selected areas of the samples. The use, however, of automatic translation stages makes easy to perform an optical and, in some cases, electrical mapping of the entire sample.
© 2002 Elsevier Science Ltd. All rights reserved.

*Keywords:* Photovoltaic materials; Optical characterization; Optical loss; Transmittance

## 1. Introduction

The optical characterization of photovoltaic (PV) materials and devices is generally limited to the use of commercial spectrophotometers. These enable the measurement of the spectral reflectance, transmittance and absorptance of any prototype sample, of small dimensions (few square centimetres), under a collimated light beam incident at a fixed angle (generally 8°). The traditional commercial optical instrumentation does not allow to change the incident angle of the light beam for the directional/hemispherical

*Corresponding author. INFM, Dipartimento di Scienze Fisiche, Università di Napoli "Federico II", Complesso Universitario di Monte S. Angelo, Via Cintia, I-80126 Napoli, Italy. Tel.: +39-081-676-126; fax: +39-081-676-346.

*E-mail address:* maddalena@na.infn.it (P. Maddalena).

($d/h$) measurements, or to use sources of diffuse light to perform hemispherical/ hemispherical ($h/h$) characterizations. Although new spectrophotometers are designed to gain more flexibility with the optical measurements, by providing them with a "testing area" to be customized for the specific optical characterization to be performed, this area has anyway to be built all over again for a new type of measurement, and only samples of small dimensions can be used, even in this case.

The knowledge of the optical behaviour of any type of PV sample either under collimated light incident at variable angles, or under diffuse light, nevertheless, would greatly contribute to the comprehension of its electrical performances when it is exposed outdoors to the solar irradiation. An aspect to face when dealing with PV samples is the fact that the final device, a PV module, differs substantially from the prototype sample characterized at the spectrophotometer. A module is provided with a glass cover sheet on its front side [1], which modifies the optical properties of the constituent unencapsulated cells and, moreover, is very large respect to a cell itself. Also the glass sheets used in the modules are generally available only as large samples, to be used directly for the encapsulation of the module. The small prototype devices, as discussed before, can be characterized at a spectrophotometer, but generally under restricted conditions as regards the angle of incidence of the light beam.

These facts have demanded the development of newly designed optical techniques for both small and large PV samples. This has been the main objective in our research work of the last years [2–14]. In this paper, we present a review of the optical techniques developed in the framework of a collaboration between ENEA laboratories and Naples University, and the results obtained characterizing both small and large PV devices at collimated and diffuse light. They demonstrate the progress achieved by us up to now in this field.

All the optical techniques here presented are non-destructive. Some of them have been patented [12–14]. These techniques permit the measurement of local areas of the samples. For prototype cells, small portions of their surface can be investigated by using laser light directed towards the area (few millimetres wide) between two adjacent fingers. The entire surface can then be investigated by moving the laser beam throughout the cell or by expanding the beam. In this last case, the effect of the grid on the measurements has to be taken into account [6,7]. The use of lamps as light sources is particularly convenient when working with the differencing reflection method (DRM) technique [8,9,13], by which the entire cell surface can be characterized in a single experiment (see the following discussion).

In the case of modules, the characterization is always limited to single cells. The cell surface is characterized by illuminating, through the glass sheet, its optically active (o.a.) region, avoiding the grid, which disturbs the measurements by its high reflectivity. The beam can be expanded to illuminate a larger portion of the cell surface. In this case, a correction to the measurements is needed to remove the grid reflection contribution [6,9]. Larger areas ($\leqslant 40\,\mathrm{cm}^2$) are exposed to light in measurements of reflectance at diffuse light following the HERE technique (see the apparatus described later on in this paragraph) [11,14]. In the characterization of integrated modules, the single cell, which appears as a long strip large about 1 cm, can be locally illuminated by a circular cross-section beam of $\sim 1\,\mathrm{cm}$ diameter.

Even local, all the described measurements can be transferred to the entire cell or module by taking their average, or by showing a map of the measurements extended to the entire device surface. This approach is the only viable when dealing with very large samples like modules or glass sheets. The characterization at solar simulator, where the entire module is illuminated, also contains information on the optical loss of the device, but this information is integrated with the others referring to the spectrum of light, level of illumination, temperature and so on. Our methods allow, on the contrary, a direct evaluation of the optical properties of the modules or of the cells, even if this entails the extrapolation of the local measurements to the entire module, by averaging or mapping procedures.

## 2. Optical characterization of modules and large PV materials

There are many aspects to the question of optical characterization of PV modules. The main aspect is related to the estimation of reflectance at collimated light. This simulates the optical loss of the module respect to the direct component of the solar radiation, that is that corresponding to the sun's disk, from which most of the total outdoor irradiation is coming at clear days. The optical loss at $0°$ incidence, $R^{dh}(0°)$, is the one experienced by the module when it is tested at a solar simulator, and is generally unknown. We have measured values of $R^{dh}(0°) \approx 4$–$9\%$ on a wide variety of commercial mono-Si modules. When the modules are installed outdoors, however, they show higher optical losses at direct light, on an average, as they are oriented towards a fixed direction (the South for the Northern Hemisphere). On the same class of modules mentioned before, we have measured 10–16% of total reflectance at $70°$ incidence.

The standard test conditions (STC) [15] protocol establishes five conditions for comparing the electrical performances of PV modules. One of these is the use of a collimated light beam for testing, incident perpendicularly to the device surface ($0°$ incidence). Respect to STC, the module develops five "energetic losses", as a consequence of the departure of the real operating conditions from those established as standard. The inverted commas are needed to indicate that the effect of a departure from standard conditions not always determines a loss [5]. For each of the five losses, it is introduced a "performance ratio" (PR) [16]. The PR related to light reflection, $PR_R$, establishes that the nominal efficiency of the module at $0°$ incidence, $\eta_{STC} = \eta_0$, should be decreased by the factor $PR_R$ when the light is incident at an angle $\theta$ [14]

$$\eta_1 = \eta_0 \, PR_R \tag{1}$$

where $PR_R$ is given by

$$PR_R = \frac{1 - R^{dh}(\theta) - A^{dh}(\theta)}{1 - R^{dh}(0°) - A^{dh}(0°)} = \frac{T^{dh}(\theta)}{T^{dh}(0°)}, \tag{2}$$

where $R^{dh}(\theta)$, $A^{dh}(\theta)$ and $T^{dh}(\theta)$ are the directional/hemispherical ($d/h$) reflectance, absorptance and transmittance of the front cover, respectively.

For this type of measurements, we have developed the apparatus "ROSE" (reflectometer for optical measurements in solar energy) [2,6,12]. Fig. 1 shows a schematic representation of the apparatus configured for reflectance measurements on PV modules. It includes a 40-cm diameter integrating sphere, an external source of light and a detector/radiometer measurement system. The integrating sphere (S) is provided with several ports (P) for the input of light at different incident angles (0°, 10°, 20°,…, 70°), distributed along the equatorial line of the sphere. Seven specular windows (A) allow to intercept the beam specularly reflected from the module. The light source (L) can be a laser or a stabilized QTH lamp. The window (W) ($d \leqslant 7.5$ cm) is provided to face the testing area of the sample (M) towards the interior of the sphere. The irradiance inside the sphere, produced by the reflected light, is measured by a silicon photodiode (D) and a radiometer (R). For spectral measurements, a filter (F) is mounted in front of the detector (D) or a monochromator is installed between the light source and the sphere.

At real operating conditions, the module is illuminated also by a distributed light (diffused or reflected), coming from the sky hemisphere or from the ground (albedo). The calculation of $PR_R$ loss factor for this illumination is not straightforward. The first approach followed by us [5,6] has been to simulate the module as a homogeneous semi-infinite dielectric with equivalent refraction index $n_{eq}$, to be experimentally determined by few $d/h$ reflectance measurements. The calculation of loss at distributed light is obtained by integrating the loss at direct light over the entire front hemisphere of the module, changing the incident angle $\theta$, the azimuth angle $\phi$ and the corresponding light intensity. Values of $n_{eq}$ have been derived [6] for many commercial mono-Si modules. Even different from each other in the internal structure (glass texturization, presence or not of an ARC layer, texturization of silicon, etc.), all the modules could be classified mainly respect to the state of the
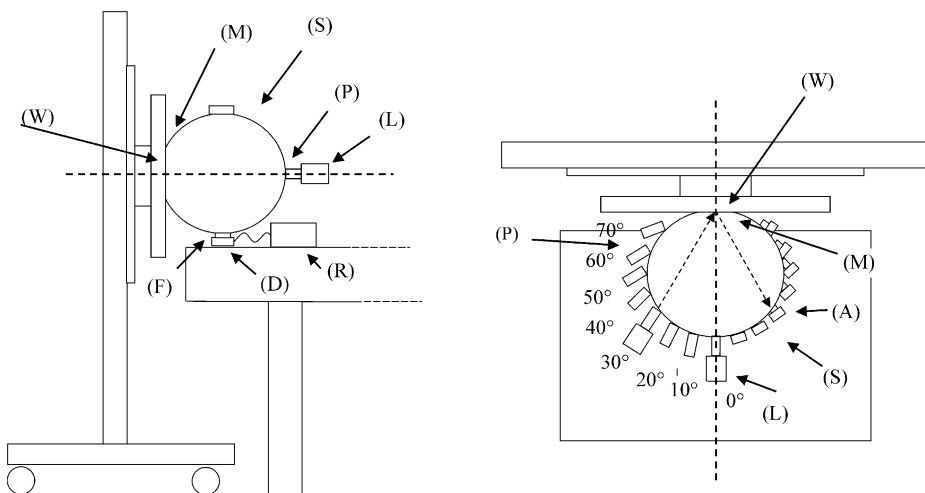


Fig. 1. Schematics of ROSE apparatus: side and top view.

glass surface. They could be modelled as dielectrics with refractive index of 2.5 or 3.0 depending only on the glass surface state, that is flat or textured, respectively.

Even if the discussed approach demonstrated to be effective, a more direct method of evaluation of the optical loss at diffuse light was desirable. This was reached by developing the reflectometer "HERE" (HEmispherical/HEmispherical REflectometer) [11,14]. It permits to make easy and rapid measurements of $h/h$ reflectance of modules at monochromatic light, $R^{hh}(\lambda)$, or at white light with spectrum "$s$", $R^{hh}(s)$. The HERE apparatus is schematically shown in Fig. 2 for the case of a laser source. Diffuse light is produced in the integrating sphere (S) by sending a collimated light beam towards the diffuser (D). The diffuse light irradiates a portion of the sample (C) which in turn reflects back into the sphere part of this light equivalent to $R_{hh}$, contributing to the irradiance inside the IS. This irradiance, measured by (R2), is a function of the average reflectivity of the internal surface of the sphere. It changes by changing the reflectivity at diffuse light of the sample (C). This simple consideration allowed us to evaluate $R_{hh}$ just by comparing the irradiance measured
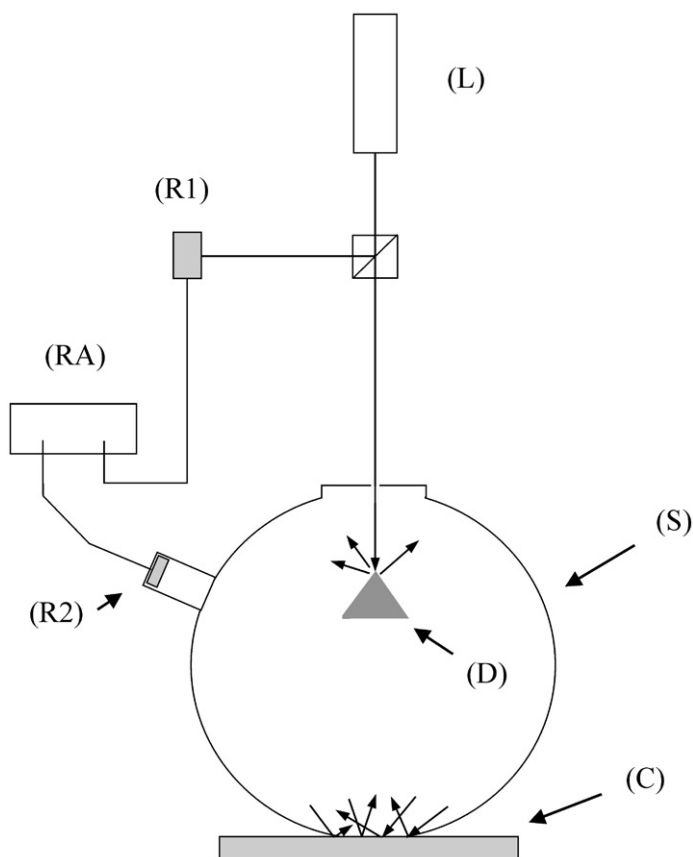


Fig. 2. Schematics of HERE apparatus.

for the sample (C) with those measured for some standards of reflectance, with known $R_{hh}$ values.

Measurements of $R^{hh}(s)$, by using a Xe arc lamp, were carried out on mono and multicrystalline silicon cells modules with different surface colorations [11,14]. $R^{hh}(s)$ values of 4–5% and 6–9% were measured for the mono-Si and m-Si cells modules, respectively.

Other aspects are related to the optical characterization of PV modules. We will briefly hereafter discuss two of them. One is the study of degradation of PV modules by using optical means. The degradation of a PV module, as due to natural exposition to the sun's light, or as obtained by simulated accelerating processes in laboratory, can be efficiently studied by measuring its reflectance before and after the degradation process. Fig. 3 shows the histogram of reflectance measured at $\lambda = 633$ nm and $10°$ incidence for a new module and for the corresponding module after a degradation process. The results of Fig. 3 have been obtained by making local measurements of $R^{dh}(10°)$ on different points of the different cells of the module. The results have been obtained by using the ROSE apparatus [4].
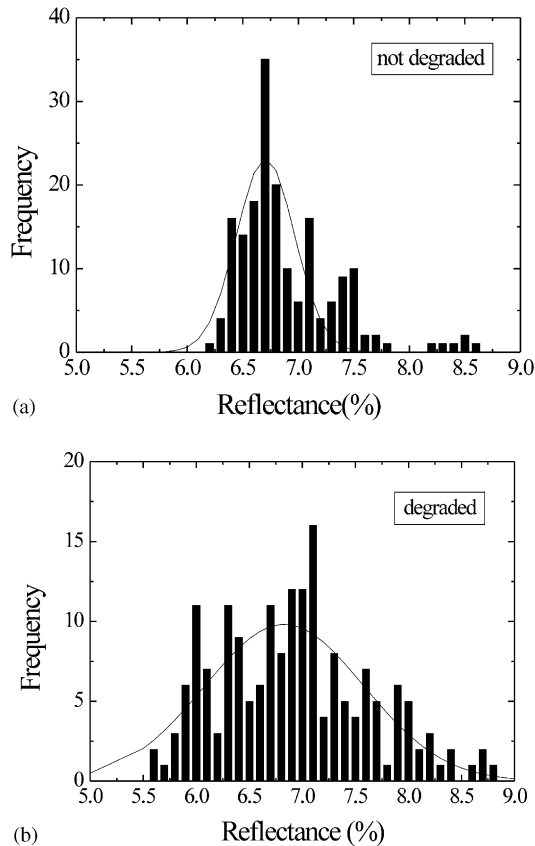


Fig. 3. Reflectance for a PV module before (a) and after (b) degradation.

The above results can be presented also as an optical map of the module, particularly when it is an integrated module (a-Si or CIS). The optical reflectance mapping (ORM) [3] technique, developed by us, gives the optical homogeneity of the layered structure. As the a-Si modules are obtained growing a-Si layers by a plasma process, the reflectance or the transmittance can put in evidence a lack in the spatial homogeneity of the layers, and then of the corresponding growth velocity. Changing wavelength, it is possible to examine this homogeneity at different depth in the cell. The ORM method is potentially very effective for the study of integrated modules performances when the optical measurements are coupled to simultaneous current measurements. The ORM mapping of a module can be carried out by providing the ROSE apparatus with a translation stage, driven by a computer, over which the module is fixed and positioned at the desired point in front of the integrating sphere.

Besides the modules, also the large glass sheets, used in their fabrication, are useful to be characterized by optical means. The glass sheet, in fact, being the first material to interact with light, has a relevant importance in the light collection. Glass sheets are prepared with one or both surfaces textured, in order to better collect both perpendicular and inclined light [17]. Useful measurements are the absorptance of glass, which directly participate to the optical loss of the module, its transmittance at variable angles of collimated light, or at diffuse light. The glass sheets can be characterized by the ROSE apparatus for $d/h$ reflectance measurements or by the HERE apparatus for $h/h$ reflectance measurements.

By providing the HERE apparatus with a supplementary, satellite sphere, it is possible to perform transmittance measurements at diffuse light, with no limits on the sample dimension (see Fig. 4) [14]. The transmittance at diffuse light, $T^{hh}(s)$, of
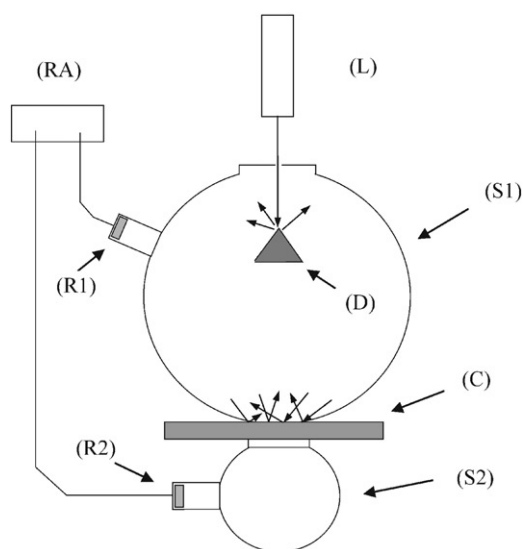


Fig. 4. The HERE apparatus equipped with the auxiliary sphere.

the sample (C) is obtained by measurements of the light transmitted from the sphere (S1) to the sphere (S2).

## 3. Optical characterization of solar cells

The ROSE apparatus was also used for the optical characterization of silicon materials and solar cells. In particular, we characterized mono-Si samples, with various surface treatments, screen-printed monocrystalline silicon (c-Si) solar cells from Eurosolare (ES), c-Si passivated emitter rear locally diffused (PERL) cells and multicrystalline silicon (multi-Si) honeycomb (HC) solar cells from UNSW [18,19]; moreover, encapsulated c-Si solar cells (EC) where used as reference samples to put in evidence the effect of the glass sheet. Fabrication details on these samples and their structure can be found in Ref. [7] and references therein.

Working with a laser (He–Ne, $\lambda = 632.8$ nm), incident on the investigated sample, maximum incidence angles of $\approx 85°$ could be reached. Conversely, by using a QTH lamp source, focused on the sample, the incidence angles were limited to $\approx 70°$.

Although the area of the metallic grid on the solar cells front surface is only a few percent of the total exposed cell area, its high reflectivity may significantly increase the overall reflectance of the device. To overcome this problem, the influence on the measured reflectance of the grid was also taken into account by means of an analytic model, which allowed subtraction of the grid reflectance on the measurements for a true sample. The validity of the model was confirmed by comparing measurements performed on PERL cells, after removal of the grid and subsequent exposure of the underlying silicon to the incident radiation, and corrected in view of the developed model, with measurements performed on "gridless" PERL cell (Fig. 5).

Measurements of reflectance on silicon materials, as a function of the incidence angle of the laser beam, showed, as expected, the highest reflectance for the polished silicon surface (Fig. 6). It was followed by the unpolished silicon, whose rough surface contributes to the light collection. A silicon sample with anti reflection coating (ARC) on its surface showed an even lower reflectance. However, the lowest reflectance values were measured for a textured silicon surface with random upright pyramids, covered by an ARC film, thanks to the so-called double bounce effect [20]; this latter effect is also responsible for the marked reflectance minimum, which the textured silicon showed at small angles, with respect to the other investigated materials, which had a flat response up to 60–70°. The measurements, if necessary, gave a further confirmation of the high efficiency of surface texturing in reducing the optical loss of a cell.

Also the total reflectance measurements on the cells showed (Fig. 7) the excellent light collection performance of the inverted pyramids structure. Indeed, the lowest values were measured for both PERL and ES cells, which had the similar texture geometry (inverted pyramids) though a different behaviour was found between the two curves of Fig. 8, for increasing incidence angles; this effect had probably to be ascribed to the different pyramids orientation with respect to the cell fingers. The EC
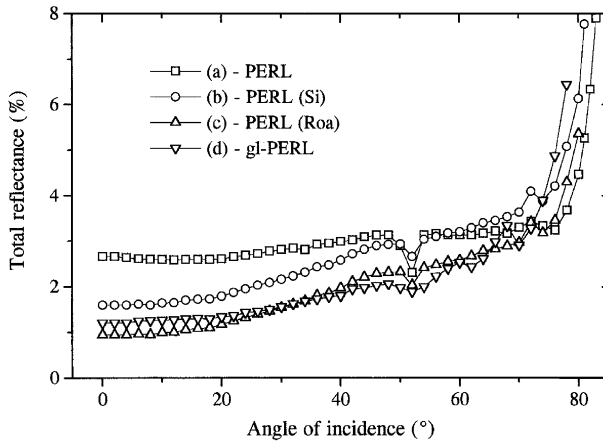
Fig. 5. Total reflectance $R_{tot}(\theta)$ at $\lambda = 632.8$ nm of the PERL cell. Curve (a) refers to measurements on the normal PERL cell; (b) to measurements on the PERL cell after removal of the metallic grid, exposing the underlying silicon; (c) is the curve obtained from (b) after correction for the silicon reflectance contribution; (d) represents the measured reflectance of a gridless cell, which is equivalent to a standard PERL cell without grid. The good agreement between (c) and (d) gives evidence of the model validity.
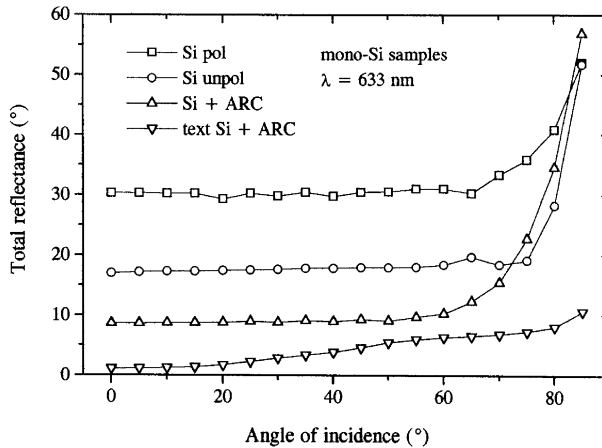


Fig. 6. Total reflectance $R_{tot}(\theta)$ at $\lambda = 632.8$ nm of mono-Si samples with different surface treatments as a function of the He-Ne laser beam incidence angle.

cell performance was, on the contrary, strongly conditioned by the presence of the glass cover sheet as for PV modules.

Spectra reflectance of the cells was studied under low irradiance conditions, too. Reflectance curves in the 400–1000 nm spectral range, for different incidence angles, showed an increased wavelength selectivity in light collection efficiency at large angles for the PERL cells (Fig. 8) as a combined result of surface texture and ARC. HC cell showed an higher reflectance in the low energy side of the investigated spectral range for both small and large incidence angles: this was ascribed in the
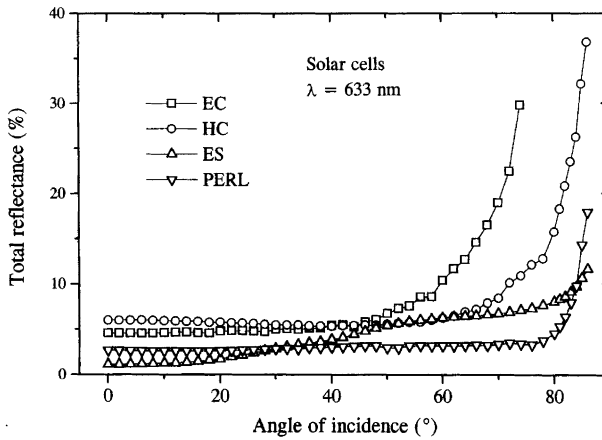
Fig. 7. Total reflectance $R_{tot}(\theta)$ at $\lambda = 632.8$ nm of four types of tested solar cells as a function of the He–Ne laser beam incidence angle.
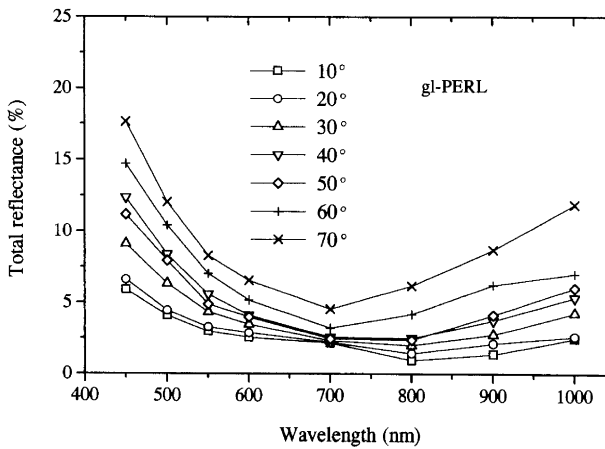


Fig. 8. Spectral reflectance $R_{tot}(\theta, \lambda)$ of the gridless PERL cell at different incidence angles of a QTH lamp light beam.

former case to the thinner wafer, which allowed reflection from the back metallic contact, and in the latter case to incident light crossing of the thin region, separating two adjacent wells of the honeycomb structure. Finally, ES cells showed a more homogeneous optical loss over the entire investigated spectrum, due to the random distribution of the upright pyramid structure.

A significant improvement, in the development of characterization techniques of solar cells, was attained introducing the DRM [8,9,13].

By this technique, limitations arising, in angle dependent reflectance measurements, from the variation of the light spot dimensions on the sample are avoided. Indeed, when a collimated light beam is incident on the sample surface, its transverse

dimension in the direction of the incidence plane increases at increasing angle of incidence: as a consequence, incidence angles have an upper limit at which the beam gets over the sample edges. Moreover, since the illuminated area changes at the different incidence angles, measurements loose significance when investigating inhomogeneous samples.

In DRM, the cell is mounted right in the centre of the integrating sphere by means of a sample holder fixed on a rotating mount in order to allow variation of the incidence angle (Fig. 9). The sample is housed in a black box, provided with a small window, through which the incoming light is incident on the sample. In this experimental configuration, the incidence angle can be varied between 0° and 90° and the exposed sample area is homogeneously illuminated. Since the system does not require reduction of the beam cross section in order to reach high values of incidence angle, the light source can be either a laser or an incoherent source such as a white light lamp, which allows easy measurements of spectral response when coupled to a proper set of band pass optical filters. A further advantage of the DRM method follows from the virtual possibility to characterize samples with very small dimensions. Finally, the contribution to the reflection from the grid eventually present on the cell surface can be taken into account analogously to what described before.

The collimated light beam is at first sent into the integrating sphere, while the sample is held up, so that the beam strikes the absorber in order to measure the background signal by the detector. The sample is then lowered so that its surface is illuminated together with a part of the box surface. Due to the low reflectivity of the black painted box, most of the reflected light comes from the sample. By comparing the irradiance measured inside the sphere when the sample is lowered, at different incidence angles, with that measured when two diffuse reflectance standards are used, the reflectance of the sample can be deduced.

In this way, the total hemispherical reflectance of a plane surface as a function of the incident wavelength or as a function of the incident angle (0°–90°) can be measured. We point out that the illuminated area of the sample is constant throughout the measurements and corresponds to the area of the box window. So
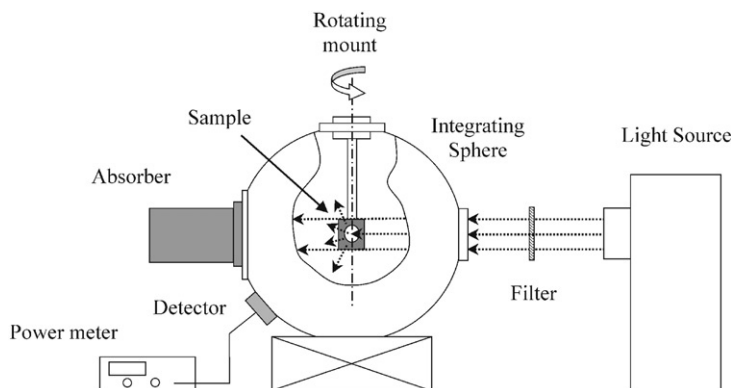


Fig. 9. Schematics of the DRM apparatus.

the measured reflectance refers always to the same region of the sample and this is a necessary requisite when investigating inhomogeneous samples.

In order to give a brief description of the principles underlying the method, we can assume that a homogeneous collimated light beam of wavelength $\lambda$ and irradiance $G_0$ is incident at angle $\theta$ on the exposed surface $S_0$ of the sample inside the box. The light power incident on the sample is then

$$P_{IC}(\theta, \lambda) = G_0 \cos \theta \, S_0.$$

If $R_C(\theta, \lambda)$ is the sample reflectance and $R_B(\theta, \lambda)$ the box reflectance, the total light power reflected into the sphere is

$$P_{BC}(\theta, \lambda) = R_C(\theta, \lambda)P_{IC}(\theta, \lambda) + R_B(\theta, \lambda)P_{IB}(\theta, \lambda),$$

where the indices C and B refer to sample and box, respectively. An analogous expression for the total reflected light power could be found when a reflectance standard is used

$$P_{BS}(\theta, \lambda) = R_S(\theta, \lambda)P_{IC}(\theta, \lambda) + R_B(\theta, \lambda)P_{IB}(\theta, \lambda).$$

By use of two reflectance standards S1 and S2 and after a little algebra, it follows that the unknown sample reflectance is given by

$$R_C(\theta, \lambda) = \frac{\Delta V_{C,S1}}{\Delta V_{S1,S2}}[R_{S2}(\theta, \lambda) - R_{S1}(\theta, \lambda)] + R_{S1}(\theta, \lambda),$$

where $\Delta V_{C,S1} = V_C - V_{S1}$ and $\Delta V_{S1,S2} = V_{S2} - V_{S1}$ represent the differences in the detector signal when it is measured for the sample, the standard S1 and S2. Similar results can be obtained in the case of white-light measurements, provided integration over the spectral range is performed for all the implied quantities.

In particular, the method was tested on a diffuse reflectance standard by comparison of the data, obtained using a traditional apparatus with an He–Ne laser beam at $\lambda = 632.8$ nm, with the ones obtained applying the DRM using a QTH lamp band-pass filtered at 650 nm. Beside the very good agreement between the two measures, DRM proved to be more stable and less affected by statistical fluctuations: both these aspects assure more precise results as found in the measurements, performed with the method, on mono-Si and honeycomb m-Si solar cells [8].

## 4. Conclusions

In this work, measurements of the optical loss of photovoltaic materials, solar cells and modules have been presented. The characterization mainly regards reflectance, both directional and hemispherical, losses; it was performed by means of different experimental apparatus, all of which are based on the use of an integrating sphere in various configurations. The proposed investigation methods are basically non-destructive and, thanks to the good signal to noise ratio attainable in the course of measurements, high sensitive to the surface conditions and morphology of the investigated samples.

# References

[1] Wenham SR, Green MA, Watt ME. Applied Photovoltaics. National Library of Australia, University of New South Wales, ISBN 0 86758 909 4, p. 69.

[2] Parretta A, Sarno A, Yakubu H. A Novel Apparatus for the optical characterization of solar cells and photovoltaic Modules. Proceedings of the Second World Conference and Exhibition on Photovoltaic Solar Energy Conversion. Wien, Austria, 6–10 July. European Commission, 1998.

[3] Parretta A, Sarno A, Pellegrino M, Privato C, Terzini E, Romano A, Yakubu H. Optical reflectance mapping (ORM): a diagnostic tool in the study of light collection in PV modules. Proceedings of the Second World Conference and Exhibition on Photovoltaic Solar Energy Conversion. Wien, Austria, 6–10 July. European Commission, 1998.

[4] Pellegrino M, Parretta A, Sarno A, Yakubu H. Detection of the encapsulant material degradation by optical measurements. Proceedings of the Second World Conference and Exhibition on Photovoltaic Solar Energy Conversion. Wien, Austria, 6–10 July. European Commission, 1998.

[5] Parretta A, Sarno A, Vicari L. Effects of solar irradiation conditions on the outdoor performance of photovoltaic modules. Opt Commun 1998;153:153–63.

[6] Parretta A, Sarno A, Yakubu H. Non-destructive optical characterization of photovoltaic modules by an integrating sphere. Part I: mono-Si modules. Opt Commun 1999;161:297–309.

[7] Parretta A, Sarno A, Tortora P, Yakubu H, Maddalena P, Zhao J, Wang A. Angle-dependent reflectance and transmittance measurements on photovoltaic materials and solar cells. Opt Commun 1999;172:139–51.

[8] Parretta A, Grillo P, Maddalena P, Tortora P. Method for measurement of the directional/hemispherical reflectance of photovoltaic devices. Opt Commun 2000;186:1–14.

[9] Parretta A, Sarno A, Maddalena P, Tortora P. A differential method for measurement of optical refectance of PV materials and devices. Proceedings of the 16th European Photovoltaic Solar Energy Conference. Glasgow, UK, 1–5 May 2000.

[10] Parretta A, Sarno A, Maddalena P, Tortora P, Yakubu H, Zhao J, Wang A. Light trapping properties of c-Si solar cells studied by reflectance and current measurements at variable angles of the incident light. Proceedings of the 16th European Photovoltaic Solar Energy Conference. Glasgow, UK, 1–5 May 2000.

[11] Parretta A, Yakubu H, Ferrazza F. Method for measurement of the hemispherical/hemispherical reflectance of photovoltaic devices. Opt Commun 2001;194:17–32.

[12] Patent IT A.N. RM 97 A 000676, 5 November 1997.

[13] Patent IT A.N. RM 99 A 000656, 25 October 1999.

[14] Patent IT A.N. RM 2000 A 000634, 1 December 2000.

[15] IEC Standards 891 and 1215, Bureau Central de la Commission Electrotechnique Internationale, Genève.

[16] Bucher K. In: Stephens HS, et al., editors. Proceedings of the 13th EC Photovoltaic Solar Energy Conference, 1995. p. 2097.

[17] Zhao J, Wang A, Campbell P, Green MA. 22.7% efficient silicon photovoltaic modules with textured front surface. IEEE Trans Electron Devices 1999;46:1495–7.

[18] Zhao J, Wang A, Altermatt P, Green MA. Twenty-four percent efficient silicon solar cells with double layer antireflection coatings and reduced resistence loss. Appl Phys Lett 1995;66:3636–8.

[19] Zhao J, Wang A, Green MA, Ferrazza F. 19.8% efficient "Honeycomb" textured multicrystalline and 24.4% monocrystalline silicon solar cells. Appl Phys Lett 1998;73:1991–3.

[20] Green MA. Silicon solar cells: advanced principles and practices. Centre for Photovoltaic Devices and Systems, UNSW, Sydney, NSW. p. 210.